Available online at www.sciencedirect.com
ScienceDirect
Journal of Power Sources 180 (2008) 205–208
JOURNAL OF POWER SOURCES
www.elsevier.com/locate/jpowsour

Short communication

High performance Pd-based catalysts for oxidation of formic acid

Rongfang Wang [a], Shijun Liao [a,*], Shan Ji [b]

[a] College of Chemistry, South China University of Technology, Guangzhou 510641, China
[b] South Africa Institute for Advanced Materials Chemistry, University of the Western Cape, South Africa

Received 20 December 2007; received in revised form 1 February 2008; accepted 1 February 2008
Available online 10 March 2008

Abstract

Two novel catalysts for anode oxidation of formic acid, Pd_2Co/C and Pd_4Co_2Ir/C, were prepared by an organic colloid method with sodium citrate as a complexing agent. These two catalysts showed better performance towards the anodic oxidation of formic acid than Pd/C catalyst and commercial Pt/C catalyst. Compared with Pd/C catalyst, potentials of the anodic peak of formic acid at the Pd_2Co/C and Pd_4Co_2Ir/C catalyst electrodes shifted towards negative value by 140 and 50 mV, respectively, meanwhile showed higher current densities. At potential of 0.05 V (vs. SCE), the current density for Pd_4Co_2Ir/C catalyst is as high as up to 13.7 mA cm^{-2}, which is twice of that for Pd/C catalyst, and six times of that for commercial Pt/C catalyst. The alloy catalysts were nanostructured with a diameter of ca. 3–5 nm and well dispersed on carbon according to X-ray diffraction (XRD) and transmission electron microscopy (TEM) measurements. The composition of alloy catalysts was analyzed by energy dispersive X-ray analysis (EDX). Pd_4Co_2Ir/C catalyst showed the highest activity and best stability making it the best potential candidate for application in a direct formic acid fuel cell (DFAFC).

Keywords: Electrocatalysts; Fuel cell; Pd-based catalysts; Formic acid oxidation

1. Introduction

Direct formic acid fuel cells (DFAFCs) have the potential for micro-power generation [1–3]. Formic acid is a liquid just like methanol, but it suffers less effects of crossover through the proton exchange membrane and has been found to have a higher rate for electrooxidation comparing with methanol [4]. Formic acid is naturally occurring, and in low concentrations is approved for use by the US Food and Drug Administration (FDA) as a food additive [5]. On the other hand, the optimal operational concentration of formic acid in DFAFCs could be as high as 15 M [6]. The power density of DFAFCs can be higher than that of direct methanol fuel cells (DMFCs), although the energy density of pure methanol is three times higher than that of pure formic acid. Thus, DFAFCs have many advantages over DMFCs.

The research on the electrocatalysts for formic acid oxidation is crucial for the development of DFAFCs. In the past several decades, many model catalysts, such as single crystal Pt [7], Pt-based metal alloy [8] and Pt modified with other metal/non-metal [9] have been investigated. Recently, it was found that Pd catalysts produced unusually high performance in active DFAFCs [10–14]. Pd not only exhibits high catalytic activity for formic acid oxidation, but also overcomes the CO poisoning effect. However, one of the disadvantages of Pd as an anodic catalyst is its instability [15].

In order to further improve the electrocatalytic activity and stability of Pd catalysts, the Pd-based alloy catalysts, such as Pd–Ni [16], Pd–Au [17] and Pd–Pd [18], etc., have been investigated. In the present work, two novel catalysts, Pd_2Co/C and Pd_4Co_2Ir/C, were prepared. Their electrochemical activity and stability for the oxidation of formic acid were much better than that of a Pd/C catalyst, especially in the case of Pd_4Co_2Ir/C.

2. Experimental

Pd_4Co_2Ir/C catalyst was prepared by an organic colloid method in an ethylene glycol (EG) solution. The detailed preparation process was described as follows: palladium chloride, cobalt chloride hexahydrate, iridium chloride and sodium citrate were dissolved in EG and then stirred for 0.5 h to completely

* Corresponding author. Fax: +86 20 87112906.
E-mail address: chsjliao@scut.edu.cn (S. Liao).

0378-7753/$ – see front matter © 2008 Elsevier B.V. All rights reserved.
doi:10.1016/j.jpowsour.2008.02.027

dissolve the citrate. Vulcan XC-72 (Carbot Corp., BET surface area: 237 $m^2\ g^{-1}$, denoted as C) carbon black (300 mg) was then added to the mixture (metal loading: 20%, and Pd:Co:Ir = 4:2:1 in atomic ratio) under stirring conditions. The pH of the system was adjusted to ~9 by dropwise addition of a 5 wt% KOH/EG solution with vigorous stirring. The mixture was placed into a Teflon-lined autoclave and then heated at 160 °C for 6 h. After obtaining the desired time, the mixture was acidified by adding 10 wt% nitric acid solution until pH of ~4 was reached, and then 5 ml of water was added, followed by sonication for 10 min. The mixture was then filtered and washed with deionized water 3–5 times, followed by drying in air at 90 °C. Finally the powders were thermally treated in a tubular oven under H_2/N_2 atmosphere at 300 °C for 2 h. The Pd_4Co_2Ir/C catalyst was thus obtained. The Pd/C and Pd_2Co/C samples were prepared in a similar procedure.

The catalysts were characterized by recording their X-ray diffraction (XRD) patterns on a Shimadzu XD-3A (Japan), using Cu Kα radiation. The mean particle size, the lattice parameter and Pd–Pd interatomic distance were calculated from the (2 2 0) diffraction plane using the Scheerer equation and the Bragg equation, respectively. The surface areas were estimated using a method from literature [19]. Transmission electron microscopy (TEM) measurements were carried out on a Tecnai G220 S-TWIN, and the acceleration voltage was 200 kV. The average chemical compositions for alloy catalysts were determined using the energy dispersive X-ray analysis (EDX) technique coupled to TEM.

The electrochemical measurements of catalysts were performed using an electrochemical workstation (Autolab, Netherlands). A common three-electrode electrochemical cell was used for the measurements. The counter and reference electrode were a platinum wire and the saturated calomel electrode (SCE), respectively. All potentials were quoted with respect to SCE. The working electrode was prepared following a previously developed technique for a high-surface area electrode [20]. The working electrode was a glassy carbon disk (5 mm in diameter), which was cleaned with deionized water, and dried in the air for the preparation of the catalyst layer on it. Briefly, the thin-film electrode was prepared as follows: 5 mg of catalyst was dispersed ultrasonically in 1 ml nafion/ethanol (0.25% nafion) for 15 min. A 4 μl portion of catalyst ink was transferred onto the glassy carbon disk using a pipette to get a Pd (Pt) loading of ~20 μg metal cm^{-2} and then dried in the air. In the electrochemical measurements, the current densities are normalized to apparent surface area of the glassy carbon electrode.

3. Results and discussion

The structure and phase analysis of the catalyst samples were performed by XRD. Fig. 1 shows the XRD patterns of Pd_4Co_2Ir/C and Pd_2Co/C catalysts with a metal loading of 20 wt%. For comparison, a Pd/C catalyst prepared with the similar procedure was also shown in this figure. The first peak located at about 24.8° in all the XRD patterns is associated with the Vulcan XC-72 carbon support. The other five peaks were characteristic of face-centered cubic (fcc) crystalline Pd (CAS number: 7440-05-3), corresponding to the planes (1 1 1), (2 0 0), (2 2 0), (3 1 1) and (2 2 2), at 2θ values of ca. 40°, 47°, 68°, 83° and 86°, respectively, indicating that all the catalysts were principally single-phase structures.

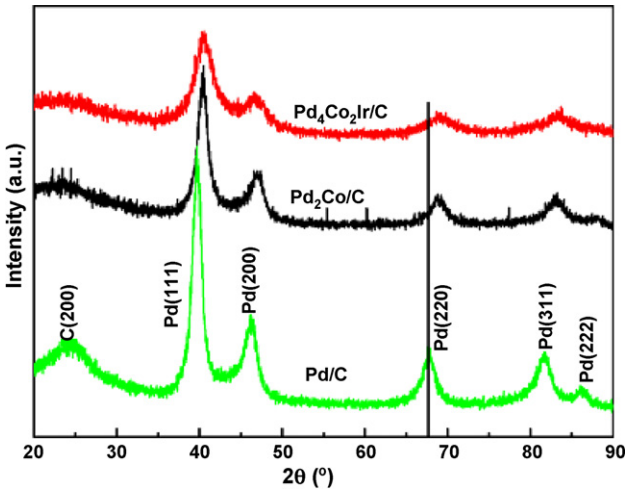

Fig. 1. XRD patterns of the Pd/C, Pd_2Co/C and Pd_4Co_2Ir/C catalysts.

The broad diffraction peaks suggested that the Pd_4Co_2Ir and Pd_2Co alloys existed in small particle sizes with a narrow size distribution. The Pd (2 2 0) crystal face had been fitted to a Gaussian line shape. The average size of the Pd particles could be calculated using Debye–Scherrer formula [21]

$$B_{2\theta} = \frac{0.94\lambda}{L\cos\theta}$$

in which $B_{2\theta}$ is the width of half peak, λ, incident wave length, L, particle diameter, θ, diffraction angle. The lattice parameters (α_{fcc}) and the Pd–Pd mean interatomic distances calculated from θ_{max} and $B_{2\theta}$ for the Pd and Pd alloys catalysts were provided in Table 1. The lattice parameter of the catalysts are in order of $Pd_2Co/C > Pd_4Co_2Ir/C > Pd/C$, indicating a lattice contraction when Co is added. The XRD-determined surface areas (S_{XRD}) were also provided in Table 1. It was reported that when the average size of Pd particles is small, the electrocatalytic activity of Pd catalyst for the formic acid oxidation is high [11]. It was found that the addition of Ir significantly improved the dispersion of the metallic components, thus increasing S_{XRD} which may enhance the activity of the catalyst.

Fig. 2 shows TEM image and corresponding EDX pattern of Pd_4Co_2Ir/C catalyst. The mean particle size could be evaluated from literature [20]. The average particle size of alloy was ca.

Table 1
Structure and mean particle size of the Pd/C, Pd_2Co/C and Pd_4Co_2Ir/C (sample) catalysts with 20 wt% metal loading

	Pd/C	Pd_2Co/C	Pd_4Co_2Ir/C
Composition from EDX	–	$Pd_2Co_{0.9}$	$Pd_4Co_{1.9}Ir_{0.1}$
Particle size (XRD) (nm)	4.8	4.3	3.5
M–M bond distance (nm)	0.2769	0.2724	0.2739
Lattice parameter (nm)	0.3916	0.3853	0.3872
S_{XRD} ($m^2\ g^{-1}$)	104.4	131.8	127.0

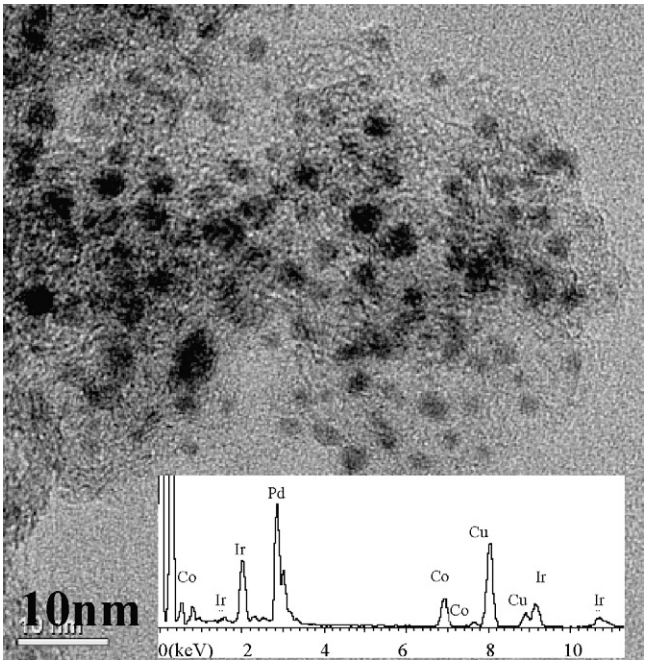

Fig. 2. TEM image and the corresponding EDX pattern of Pd_4Co_2Ir/C catalyst.

3.5 nm, which was in good agreement with that from the above XRD measurement. The average particle size of Pd_4Co_2Ir was smaller than other Pd-based catalysts, which might be beneficial for increasing the activity of formic acid oxidation. The composition of carbon supported Pd_4Co_2Ir alloy electrocatalysts was determined by EDX analysis. The elemental analysis by EDX was shown in Table 1 and the insert of Fig. 1. It was found that EDX composition of the prepared catalyst was close to the nominal value.

Fig. 3 plots the cyclic voltammograms of Pd_4Co_2Ir/C, Pd_2Co/C and Pd/C catalysts in 0.5 M H_2SO_4 under N_2 atmosphere. The Pd/C exhibited a large hydrogen peak below 0.1 V versus SCE. This large peak was caused by dissolution of the adsorbed hydrogen into the bulk of the Pd electrode.

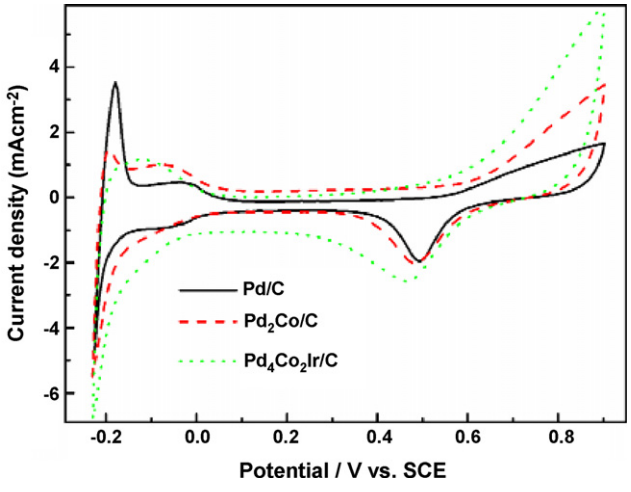

Fig. 3. Cyclic voltammograms of Pd_4Co_2Ir/C, Pd_2Co/C and Pd/C catalysts in 0.5 M H_2SO_4 under N_2 atmosphere; scan rate = 50 mV s^{-1}, rotation speed = 300 rpm, 25 °C.

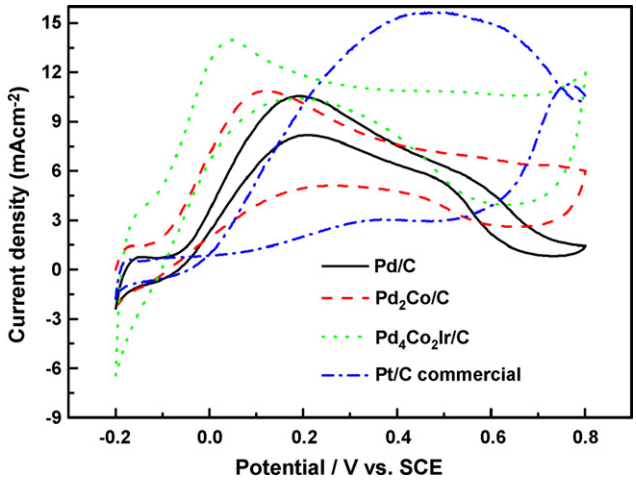

Fig. 4. Cyclic voltammograms of 0.5 M HCOOH in the 0.5 M H_2SO_4 solution on the Pd_4Co_2Ir/C, Pd_2Co/C, Pd/C and Pt/C electrodes; scan rate = 50 mV s^{-1}, rotation speed = 300 rpm.

The Pd_4Co_2Ir/C and Pd_2Co/C electrocatalysts showed different hydrogen peaks compared to the Pd/C. Since Pd/C exhibited a poor definition of the hydrogen region, the quantity of electric charge used in the reduction of palladium oxide formed over the top layer of the Pd particles, probably as a form of PdO, was employed in calculating the specific surface area [17]. From Fig. 3 we found that the oxide reduction peak of Pd_4Co_2Ir/C was bigger than that of Pd_2Co/C and Pd/C, which was in agreement with the result from XRD.

Fig. 4 shows the cyclic voltammograms of 0.5 M HCOOH in the 0.5 M H_2SO_4 solution on the Pd_4Co_2Ir/C, Pd_2Co/C, Pd/C and Pt/C (Johnson–Matthey, 20 wt% metal loading) electrodes. It was reported that the oxidation of formic acid on the Pd catalyst is mainly through the direct pathway [1]. The current density of the peak at 0.1–0.2 V (through the direct pathway) is much larger than that at 0.5–0.6 V (through the CO pathway). It could be observed from Fig. 4, that the oxidation of formic acid for the prepared catalysts was mainly through the direct pathway, too.

In comparison with the Pt/C catalyst, the potential of the main peak for the oxidation of formic acid on the Pd_4Co_2Ir/C electrode shifted about 700 mV in the negative direction. For the Pd/C catalyst, the potential of the main peak for the oxidation of formic acid on the Pd_4Co_2Ir/C electrode shifted 140 mV in the negative direction and the peak current density was increased by 3.64 mA cm^{-2}. For the Pd_2Co/C catalyst electrode, the main peak of formic acid oxidation shifted about 50 mV towards negative values and the peak current density was increased by 0.31 mA cm^{-2}. Because the average sizes of the Pd and Pd-alloy particles in the Pd_4Co_2Ir/C, Pd_2Co/C and Pd/C catalysts are different, the peak current density could be corrected by S_{XRD}. Compared to Pd/C catalyst, the corrected peak current for the Pd_4Co_2Ir/C catalyst increased 1.2 times and Pd_2Co/C catalyst decreased 1.1 times. On the other hand, it was also reported that the main anodic peak of formic acid at Pd–Ir/C was only 50 mV more negative than that of Pd/C catalyst [22]. Those results illustrated that the high electrocatalytic activity of the Pd_4Co_2Ir/C catalyst could be attributed to the Ir and Co doping.

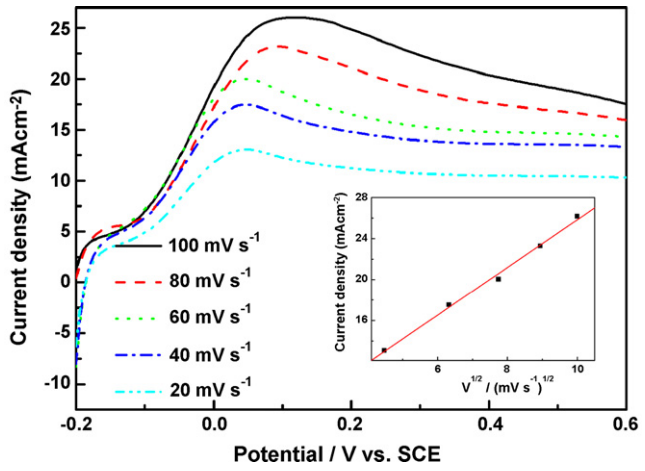

Fig. 5. The linear sweep voltammetry curves for formic acid oxidation on Pd_4Co_2Ir/C electrode at different scan rate. The dependence of peak current on scan rates is shown in the insert.

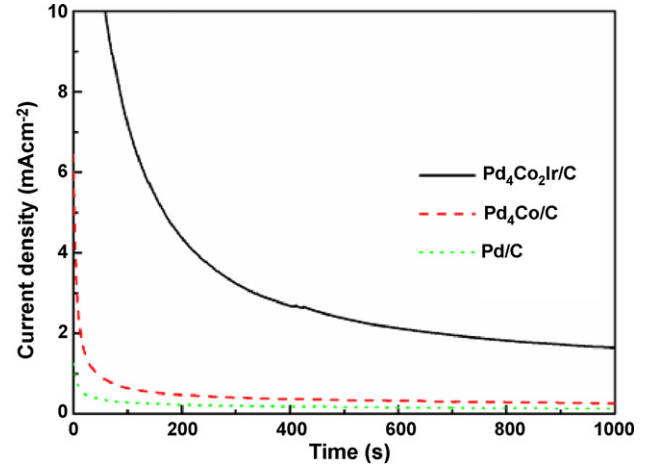

Fig. 6. The chronoamperometric curves of 0.5 M HCOOH in 0.5 M H_2SO_4 solution on Pd_4Co_2Ir/C, Pd_2Co/C and Pd/C electrodes for 1000 s; fixed potential = 0.1 V, rotation speed = 600 rpm.

We can also compare their activities at a constant potential, at potential of 0.05 V (vs. SCE), the current densities for catalysts Pt/C, Pd/C, Pd_2Co/C and Pd_4Co_2Ir/C are 2.2, 5.5, 8.5 and 13.7 mA cm^{-2}, respectively. It is clear that the activity of Pd_4Co_2Ir/C catalyst is six times of that of Pt/C catalyst, and twice of that of Pd/C catalyst.

In order to investigate the kinetic characterization of formic acid oxidation on Pd_4Co_2Ir/C electrode, we looked into the effect of scan rate on the behavior of formic acid oxidation. Fig. 5 shows the cyclic voltammograms of the Pd_4Co_2Ir/C electrode at different scan rates. The scan was performed with five cycles to obtain the stable response and the last cycle is shown in Fig. 5. The peak current increases linearly with the square root of the scan rates as shown in Fig. 5 insert. This indicates that the electrocatalytic oxidation of formic acid on Pd_4Co_2Ir/C-modified electrode is a diffusion-controlled process.

Fig. 6 shows the chronoamperometric curves of 0.5 M HCOOH in 0.5 M H_2SO_4 solution on Pd_4Co_2Ir/C, Pd_2Co/C and Pd/C electrodes at 0.1 V. It could be observed from Fig. 6 that the current densities on the Pd_4Co_2Ir/C, Pd_2Co/C and Pd/C electrodes at 1000 s were 2.02, 0.24 and 0.11 mA cm^{-2}, respectively. The above results demonstrated that the electrocatalytic stability of the Pd_4Co_2Ir/C catalyst for formic acid oxidation is much higher than that of the Pd_2Co/C and Pd/C catalysts.

4. Conclusion

In summary, two novel catalysts Pd_2Co/C and Pd_4Co_2Ir/C for formic acid oxidation were synthesized by an organic colloid method. TEM and XRD characterizations showed that the obtained catalysts had a smaller particle size and highly dispersed alloy nanoparticles on the carbon support. The electrochemical results demonstrated that the catalytic performance of these catalysts for the oxidation of formic acid and the catalytic stability were improved remarkably with the addition of Ir and Co.

Acknowledgments

We would like to thank the State Natural Science Foundation of China and Guangdong Provincial Natural Science Foundation for their financial support in this work (Project Nos. 20476034, 20673040, 03665).

References

[1] S. Ha, R. Larsen, Y. Zhu, R.I. Masel, Fuel Cells 4 (2004) 337.
[2] C. Rice, S. Ha, R.I. Masel, P. Waszczuk, A. Wieckowski, T. Barnard, J. Power Sources 111 (2002) 83.
[3] H. Li, G. Sun, Q. Jiang, M. Zhu, S. Sun, Q. Xin, Electrochem. Commun. 9 (2007) 1410.
[4] S. Ha, Z. Dunbar, R.I. Masel, J. Power Sources 158 (2006) 129.
[5] US Code of Federal Regulations, 21 CFR 186.1316.
[6] C. Rice, S. Ha, R.I. Masel, A. Wieckowski, T. Barnard, J. Power Sources 115 (2003) 229.
[7] R.R. Adzic, A.V. Tripkovic, W. O'Grady, Nature 296 (1982) 137.
[8] S. Sun, Y. Yang, J. Electroanal. Chem. 467 (1999) 121.
[9] X. Li, I. Hsing, Electrochim. Acta 51 (2006) 3477.
[10] S.Y. Ha, R. Larsen, R.I. Masel, J. Power Sources 144 (2005) 28.
[11] P.K. Badu, H.S. Kim, J.H. Chung, E. Oldfield, A. Wieckowski, J. Phys. Chem. B 108 (2004) 20228.
[12] X.G. Zhang, A. Toshihide, M. Yasushi, Y. Kiyochika, T. Yoshio, Electrochim. Acta (1995) 1889.
[13] Y.M. Zhu, K. Zakia, R.I. Masel, J. Power Sources 139 (2005) 15.
[14] L. Zhang, T. Lu, J. Bao, Y. Tang, C. Li, Electrochem. Commun. 8 (2007) 1625.
[15] K. Persson, A. Ersson, N. Iverlund, S. Jaras, J. Catal. 231 (2005) 15.
[16] T. Shobha, C.L. Aravinda, P. Bera, L.G. Devi, S.M. Mayanna, Mater. Chem. Phys. 80 (2003) 656.
[17] M. Baldauf, D.M. Kollb, J. Phys. Chem. 100 (1996) 11375.
[18] F.S. Thomas, R.I. Masel, Surf. Sci. 573 (2004) 169.
[19] J.L. Fernandez, D.A. Walsh, A.J. Bard, J. Am. Chem. Soc. 127 (2005) 357.
[20] R.F. Wang, S.J. Liao, H.Y. Liu, H. Meng, J. Power Sources 171 (2007) 471.
[21] E. Antolini, F. Cardellini, J. Alloy Compd. 315 (2001) 118.
[22] X. Wang, Y. Tang, Y. Gao, T. Lu, J. Power Sources 175 (2008) 784.